



ORIGINAL RESEARCH PAPER

Engineering

INFLUENCE OF ENERGY AND DOSE OF IMPLANTED IONS ON THRESHOLD VOLTAGE OF MOS STRUCTURE

KEY WORDS:

Anil Kumar

Naina Semiconductor Ltd ,noida.

G. S. Viridi*

GS Collage Of Modern Technology,kharar, Mohali. *Corresponding Author

ABSTRACT

This work carried out with a view to study the variation of threshold voltage of MOS structure grown on non-uniformly doped substrate. The authors have used ion-implantation as a method of growing non-homogeneously doped layer on silicon substrate. Boron implantation in p-type substrate with different doses of Boron ions, varying from 1×10^{12} ions/cm² to 1×10^{15} ions/cm² and energies 20Kev to 120Kev is considered, which provides a variety of impurity profiles in the substrate. Capacitance-Voltage curves have been obtained from the numerical solution of Poisson's equation. The threshold voltage has been assumed to be given by voltage applied to the gate of MOS structure at which strong inversion take place. This has been observed that as the energy of the implanted ions is increased, keeping the dose fixed at 1×10^{14} ions/cm², the threshold voltage of MOS capacitor fabricated on this substrate decreases. where as when the dose of the Boron implanted ions is increased, keeping the energy fixed at 50Kev, the threshold voltage increases. Thus the threshold voltage of MOS capacitor not only be controlled by the Dose of the implanted ions in the substrate but also by the energy of the implanted ions, because both these parameters bring about changes in impurity concentration profiles in the substrate.

INTRODUCTION:

Introduction of impurities in silicon is an important feature in LSI and VLSI technology. The electrical characteristics of semiconductor are primarily determined by the impurities incorporated into the body of the semiconductor. For example sheet resistance of dopant substrate depends on the profile of net dopant in substrate [1]. The sheet resistance of silicon with mixed implantation of dopant also depend on the distribution of the dopant species [2-3]. Threshold voltage of MOSFET can be varied by varying the distribution of impurities near the surface of substrate. The distribution of impurities in the substrate has significant effect on the characteristics of devices fabricated on such substrates.

S.D.Brotherton et al [4] have shown that for non-uniformly doped substrate the theoretical C-V curve can be significantly different from the theoretical C-V curve having the same minimum capacitance, but assumed to be grown on uniformly doped substrate. Brotherton et al [4] have numerically calculated the theoretical MOS CV curves for an exponential acceptor type profile in a p-type substrate. Ion-implantation technique has been employed to control the threshold voltage [5] of MOS transistors because ion implantation produces non uniform doping profiles close to the silicon surface.

M.R.Macpherson [6] carried out C-V calculations for Boron implanted the SiO₂-Si(n-type) system assuming a Gaussian distribution of impurities and showed that the measured C-V curves qualitatively agree with the theoretical data. In his calculation he varied the energy and the thickness of the oxide layer in order to keep the peak of the implanted impurity profile at the SiO₂-Si interface and varied the energy while keeping the oxide thickness fixed to shift peak of the impurity concentration profile inside the substrate. In the latter case he observed the saturation in the threshold voltage at higher energy.

Doucet et al [7] have derived a semi-analytical expression for the MOS C-V curves and threshold voltage and made an explicit comparison with the numerical solution for the specific case of an exponential profile.

Edward.C.Douglas et al [8] presented an analytical model based on the thermal diffusion of an initially ion-implanted impurity profiles and used this as a guide in the study of threshold voltage control.

Ronald R.Troutman [9] developed an analytical expression for the threshold voltage of a long channel MOSFET with a ion-implanted profiles. Impurity concentration profiles of boron implantation was considered which was subjected to high temperature annealing as a result of which the peak of impurity

concentration shifts to SiO₂-Si interface. A good agreement between theoretical and experimental results was observed over a wide range of implant conditions and background doping.

J.R.Brews [10] gave a new criterion for threshold voltage shift due to implantation as the shift in the curves of N_{inv} versus V_G where N_{inv} is the inversion layer carrier density per unit area and V_G is the gate voltage of the MOSFET. He introduced a simplified method of calculation to evaluate N_{inv} and V_G without using the numerical solution of Poisson's equation.

S.W.Tarasewicz et al [11] carried out work on the calculation of high frequency C-V curves of MOS capacitors with the non uniformly doped substrate by using depletion approximations. The impurity profiles were approximated by a straight line near the SiO₂-Si interface with these approximations high frequency C-V curves were developed and tested on the devices with implanted impurity profiles. A very good agreement between the theoretical and experimental results was observed over the depletion and inversion regions. They have considered the impurity profiles whose concentrations varies very slowly with depth e.g from 1×10^{16} atoms/cm³ to 2×10^{16} atoms/cm³.

In the present work the authors have carried out work on the calculation of C-V curves on the Ion Implanted substrate having steep shallow ion-implanted impurity profiles with implantation dose varying over a wide range. C-V curves have been obtained from the numerical solutions of Poisson's equations.

Since Ion-Implantation affects the threshold voltage of MOS structure by introducing additional impurity ions in the depletion layer which modify the nature of voltage dependence of the depletion layer. Threshold voltage here means the voltage applied to the gate of MOS structure at which strong inversion takes place. It is interesting to see the effect of energy and dose of the implanted ions on the threshold voltage, as both these parameters modify the depletion width by introducing in it the impurity ions. It may be noted that by varying the dose for a given energy of implanted ions, surface impurity concentration as well as peak concentration of implanted impurities vary, position of peak remaining the same. Alternatively keeping the implanted ions dose fixed and varying the energy the surface concentration, peak concentration and peak position varies. In the present work different types of impurity profiles have been considered. Boron dose 10^{12} to 10^{15} atoms/cm² and energies 20Kev to 120Kev considered for variety of profiles. Earlier most of the workers have carried out work by doing implantation through SiO₂ grown on Si and most of them have attempted to keep the peak of implanted profile at SiO₂-Si interface.

In the present work SiO₂ is assumed to be grown on the implanted

substrate and various possible positions and heights of dopant profile distribution are considered near the surface of the silicon substrate. Low frequency C-V curves are then derived from the numerical solution of Poisson's equations.

Threshold voltage and high frequency C-V curves are then derived from these low frequency C-V curves.

For the profiles considered, it has been observed that the threshold voltage increases as the dose of the implanted ions increases, when the energy of the implanted ions kept fixed. When the energy of the implanted ions is allowed to increase, keeping dose fixed, the threshold voltage, however, decreases for the impurity profiles considered.

The authors have made an attempt to explain these variations by taking into consideration the nature of depletion layer width dependence on applied voltage under different conditions of implantation. Present results on the threshold voltage calculations are also compared with the results obtained by using linear approximation [11]. In order to verify the effect of energy and dose on the threshold voltage, the MOS capacitors were fabricated on the ion-implanted substrates and threshold voltage was calculated from these high frequency C-V curves.

Study of literature reveals that the cases considered by the authors in the present work have not been reported by the other investigators so far. Some of the results presented by the authors, namely the possibility of threshold voltage decrease or increase and nature of variation etc. under certain conditions of implantation, do not find mention in the published literature in the manner the authors have discussed. The authors have considered the MOS structure grown on an ion-implanted silicon substrate as against implanted SiO₂-Si system considered by most of the investigators mentioned in the introductory review.

MOS C-V CURVE ANALYSIS:

In order to calculate MOS C-V curves one has to solve Poisson's equation for surface potential as a function of surface charge density.

The Poisson's equation to be solved is

$$\frac{d^2\psi}{dx^2} = -\frac{\rho(x)}{\epsilon_s} \dots\dots 1$$

The space charge density

$$\rho(x) = q(p-n-N_A(x)) \dots\dots\dots 2$$

Considering surface doped with acceptor impurities NA(x). NA(x) is assumed to be given by Gaussian distribution of the form indicated by equation 3, which gives the concentration of implanted atoms at the depth x from the surface. The values of projected range, RP, and standard deviation, ΔRp, are substituted in this equation for given values of energy. The impurity concentration profile can thus be obtained for a given value of dose D, and energy implantation

$$N_A(x) = \frac{D}{\sqrt{2\pi}\Delta R_p} e^{-\frac{(-1/2(x-R_p))^2}{(\Delta R_p)^2}} + N_A(SUB) \dots\dots\dots 3$$

Using Boltzman statistic, the free carrier concentration are given by

$$p = n_i e^{(q(\psi_b - \psi)/KT)} \dots\dots\dots 4$$

$$n = n_i e^{(q(\psi - \psi_b)/KT)} \dots\dots\dots 5$$

substituting 3,4,5 into 1 one get

$$\frac{d^2\psi}{dx^2} = -\frac{2n_i q}{\epsilon_s} \left[\sinh \frac{q}{KT} (\psi_b - \psi) - \frac{N_A(x)}{2n_i} \right] \dots\dots\dots 6$$

This equation is solved numerically to get Ψ_s and dΨ_s/dx at a surface using fourth order Runga Kutta method [12].

The field ES and as a function of surface potential Ψ_s is then obtained from

$$E_s(\Psi_s) = -\frac{d\psi_s}{dx} \dots\dots\dots 7$$

Similarly, by Gauss's law the space charge density required to produce this field is given as

$$Q_s(\Psi_s) = \epsilon_s E_s(\Psi_s) \dots\dots\dots 8$$

The differential capacitance of the semiconductor space charge is given by

$$C_D(\Psi_s) = \frac{dQ_s}{d\psi_s} \dots\dots\dots 9$$

The total capacitance of the MOS capacitor is a series combination of the oxide layer capacitor and the silicon space charge capacitance C_D

$$C(\Psi_s) = \frac{C_{ox} C_D}{C_D + C_{ox}} \dots\dots\dots 10$$

In a practical MOS capacitor, the silicon surface charge is varied by changing the potential, V_G on the metal electrode and V_G also can be expressed as a function of Ψ_s by [13]

$$V_G = \psi_s - \frac{Q_s(\Psi_s)}{C_{ox}} \dots\dots\dots 11$$

For various values of Ψ_s, equation 6 is solved to get dΨ_s/dx and by using equation 7 the field E_s is calculated. Space charge density required to produce this field is calculated using equation 8. From the data of space charge density and surface potential the slope is taken at each point of Ψ_s to obtain space charge capacitance using equation 9. For a given value of oxide layer capacitance COX, and the space charge capacitance, the total capacitance of MOS is calculated.

In the present work in order to solve equation 6, Runga-Kutta method has been employed. Initial values of Ψ, dΨ/dx and N_A are calculated at a particular values of x. These values are obtained by the method described below.

Impurity concentration N_A(x) is calculated by using equation 3 for a given depth x. Assuming that the number of free carriers is equal to number of impurity atoms i.e. p = N_A(x), potential Ψ(x) is calculated by Substituting values of p and N_A(x) from equations 3 and 4. After rearranging the terms, the potential is found to be equal to

$$\Psi = \psi_b - \frac{KT}{q} \ln \frac{1}{n_i} \left[\frac{D}{\sqrt{2\pi}\Delta R_p} e^{-\frac{(-1/2(x-R_p))^2}{(\Delta R_p)^2}} + N_A(SUB) \right] \dots\dots\dots 12$$

dΨ/dx is obtained from equation 12 as

$$\frac{d\psi}{dx} = \frac{D}{\sqrt{2\pi}\Delta R_p} e^{-\frac{(-1/2(x-R_p))^2}{(\Delta R_p)^2}} \frac{x-R_p}{(\Delta R_p)^2} \dots\dots\dots 13$$

From these values of N_A(x), Ψ and dΨ/dx equation 6 is solved to obtain values of Ψ_s and dΨ_s/dx.

In this manner for various given values of Ψ_s, equation 6 is solved to obtain dΨ_s/dx and C-V curves are obtained. These calculations are then repeated for various types of impurity profiles corresponding to the given energy of implantation and dose. These are obtained by putting appropriate values of R_p and ΔR_p in equation 3. Table 1 and table 2 give various energies and doses of boron as implanted ions and their corresponding R_p and ΔR_p values. The values of R_p and ΔR_p are taken from the published data [14], calculated on the basis of Lindhard, Scharff and Schiøff (LSS) Theory [15].

For the above mentioned calculations of C-V curves the thickness of oxide layer grown on the implanted substrate has been assumed to be 1000 Å and uniform background substrate concentration N_A(sub) has been assumed to be equal to 1x10¹⁵ atoms/cm³. Figure 1 and 2 show the impurity concentration profiles of boron implanted in silicon, with uniform background concentration of 1x10¹⁵ atoms/cm³, for which the C-V curves calculations are made. Fig 1 Shows the profiles, when dose is kept fixed at 1x10¹⁴ ions/cm² and energy varied from 20Kev to 120Kev.

Fig.2 shows the profiles, when energy is kept fixed at 50Kev and dose is varied from 1x10¹² ions/cm² to 1x10¹⁵ ions/cm². These

profiles are calculated by using equation 3 for various values of R_p , a ΨR_p , Representing energies and doses given in table 1 and 2.

Solving equation 6, the field E_s as a function of surface potential Ψ_s is calculated which by using equation 8 is converted into charge density Q_s as a function of Ψ_s .

Fig 3 and Fig4 show the plots of space –charge density versus surface potential, numerically calculated for profiles of Fig 1 and Fig 2 respectively. Curve 8 in figure 3 and 5 in fig.4 represent the plots for an implanted uniformly doped substrate with doping concentration of 1×10^{15} atoms/cm³. This has been done to compare the results of implanted and un implanted substrates. The capacitance versus voltage curves obtained for these profiles are shown in Fig 5a and Fig 6a, by using equations 9, 10 and 11. Fig 5b show the details of curve 8 of Fig 5a and Fig 6b show the details of curve 5 of Fig 6a.

Low frequency C-V curves have been obtained because in the calculations charge in the inversion region is assumed to follow variation in applied potential. In order to derive high frequency C-V curves from low frequency C-V curves, obtained theoretically, threshold voltage for each curve is calculated by making use of Fig 3 and Fig 4. giving variation of Q_s versus Ψ_s . As shown in Fig 3, curve 1, the quasi-linear portion of the curve corresponding to depletion and weak inversion A, and the linear portion of the strong inversion B are extrapolated to meet at appoint. This point is assumed to indicate onset of strong inversion and therefore, correspond to threshold voltage.

Oxide layer capacitance is calculated for 1000Å^o oxide layer grown on implanted substrate by using the formula $C_{ox} = \frac{\epsilon_{ox}}{t_{ox}}$. In order to calculate high frequency C-V curves, a line parallel to y-axis is drawn at a voltage point on x-axis corresponding to threshold voltage, calculated by the method mentioned above. The portion of C-V curves, corresponding to depletion region is extrapolated to meet this threshold voltage. Capacitance corresponding to that point is kept constant, because threshold voltage represents that voltage at which inversion in MOS capacitor takes place and total capacitance of MOS capacitor achieved its minimum value and remain constant. Fig. 5 and Fig6 also show the high frequency C-V curves derived from the low frequency C-V curves.

Maximum depletion width can be calculated from C_{min} capacitance where C_{min} is the capacitance of MOS capacitor at threshold voltage.

$$C_{min} = \frac{C_{ox} C_{DT}}{C_{ox} + C_{DT}} \dots\dots\dots 14$$

Where C_{DT} is the space charge capacitance at threshold voltage C_{DT} can be written as

$$C_{DT} = \frac{C_{min}}{1 - \frac{C_{min}}{C_{ox}}} \dots\dots\dots 15$$

From equation 15 maximum depletion width can be written as

$$W_{max} = \frac{\epsilon_s}{C_{DT}} \dots\dots\dots 16$$

C_{DT} can be calculated from the knowledge of C_{ox} and C_{min} . W_{max} is calculated for all the C-V curves. In the similar way these calculations are performed for different C-V curves. The average impurity concentration within the W_{max} depletion region is calculated using the method followed by S.W.Tarasewicz et al calculations.

From all the results shown in table 3 it is observed that as the energy of the implanted ions increases for the fixed value of dose, the maximum width of the depletion layer increases. This is because as the energy increases, the peak of the impurity profile penetrate deeper and deeper and the average impurity concentration in the depletion layer decreases, which result in an increase in the depletion layer width. Because of the decrease in average impurity concentration in the depletion layer with increase

in implantation increase in implantation energy, the threshold voltage decreases. In table 4, it is observed that as the dose of the implanted ions vary for a given value of energy, the depletion layer width decreases, because the average impurity concentration in the depletion layer increases, so the threshold voltage increases as the dose increases.

In order to verify the results obtained by the numerical analysis of Poisson's equation, the results are compared with those obtained by using the method of calculations followed by S.W. Tarasewicz et al. based on depletion approximation. Threshold voltage, maximum depletion layer width and average impurity concentration are calculated for the similar cases of implanted ions into p-type silicon by the method proposed by S.W. Tarasewicz et al. applied the depletion approximation to the semiconductor with linearly graded impurity profile. Impurity profiles were approximated by a straight line near the SiO₂-Si interface. The distribution of the electric field and potential in depletion region were found and the relationship between the surface potential and depletion width was obtained. High frequency C-V curve

Was then obtained. In their work they have considered n-type impurities in silicon. Assuming impurity concentration profile approximated by straight line near the SiO₂-Si interface, given by

$$N_D(x) = N_s + MX \dots\dots\dots 17$$

Impurity gradient, M , can be either negative or positive, depending on the profile at SiO₂-Si interface. Both the parameters N_s and M are determined from the best fit to the original profile over the expected maximum width of the surface depletion layer.

The Poisson's equation to be solved is

$$\frac{d^2 \psi}{dx^2} = - \frac{q(N_s + MX)}{\epsilon_s} \dots\dots\dots 18$$

After subjecting to two boundary conditions suggested by S.W. Tarasewicz et al. defining the electric field and the potential at the end of surface depletion region, W , as

$$E(w) = \frac{V_t M}{N_s + MW} \dots\dots\dots 19$$

Where V_t is thermal voltage, and

$$\psi(w) = V_t \frac{(N_s + MW)}{N_D(SUB)} \dots\dots\dots 20$$

The surface potential Ψ_s is given by

$$\Psi_s = - \frac{qW^2}{\epsilon_s} \left[\frac{N_s}{2} + \frac{MW}{3} \right] V_t \left[\ln \left(\frac{N_s + MW}{N_D(SUB)} \right) - \frac{MW}{N_s + MW} \right] \dots\dots\dots 21$$

At strong inversion, the surface minority carrier concentration is equal to the minority carrier concentration is equal to the majority carrier concentration at the boundary of depletion layer.

The surface potential corresponding to this condition is given as

$$\frac{\Psi_s}{inv} = V_t \ln \left[\frac{n_i^2}{N_D(w) N_D(SUB)} \right] \dots\dots\dots 22$$

From equation 21 and 22, the maximum depletion width can be calculated. For an ideal MOS capacitor, Fabricated on n-type substrate, the gate voltage is expressed as

$$V_G = - \frac{Q_s}{C_{ox}} + \Psi_s \dots\dots\dots 23$$

For p-type substrate, the gate voltage is given by equation 11 S.W. Tarasewicz et al have expressed Q_s in the form

$$Q_s = q \int_0^{W_{max}} (N_s + MX) dx - \int_0^{W_{max}} \frac{\epsilon_s V_t M^2}{(N_s + MX)^2} + \frac{\epsilon_s V_t M^2}{N_s} \dots\dots\dots 24$$

Q_s is the charge distribution under the depletion condition in uniformly doped substrate. W_{max} is the maximum depletion width which can be calculated from equation 21 and 22. The space charge density Q_s can be calculated by putting the value of W_{max} into equation 24 and gate voltage can be calculated by using equation 23. Where Ψ_s is Ψ_{sin} in this equation, this gate voltage is

the threshold voltage of the MOS capacitor. The average impurity concentration within W_{max} can be calculated from the relation

$$N_{av} = \frac{1}{W_{max}} \int_0^{W_{max}} (N_s + MW) dW \dots\dots 25$$

The authors have carried out calculations for boron implantation into p-type substrate against the S.W. Tarasewicz et. al. calculations in which they have considered n-type impurities into n-type substrate, so the sign in the calculation has been taken into consideration. All the impurity concentration profiles are approximated by a straight line up to the expected maximum depletion width by using the method of least square line fitting. The values of the surface concentration, N_s , and the impurity gradient M are calculated by this method. It has been observed that the surface concentration, N_s , assumed negative sign for some cases, table 5 and table 6, but when these values are substituted to calculate W_{max} , N_{av} , V_t , etc., the results obtained by the numerical analysis method. Negative sign of N_s is simply a parameter representing linear approximation to the actual profile, and therefore does not represent the actual value of surface concentration. The values of N_s and M are then substituted in equation 21 and 22 the W_{max} is calculated. Solving equation 24 and 25 by substituting the W_{max} and by making use of equation 23, the threshold voltage and average impurity concentration are calculated. In a similar manner the average impurity concentration within W_{max} are calculated, the values calculated for N_s, M, N_{av}, V_t and W_{max} are given in tables 5 and 6, for corresponding energy and dose of the boron implanted into p-type substrate (background impurity concentration 1×10^{15} atoms/cm³ and 1000Å² oxide layer grown on this substrate)

EXPERIMENT

In order to study the effect of a variety of implantation schedule on the MOS C-V curves experimentally, MOS capacitors were fabricated on the implanted substrate. Boron implantation was carried out using Kasper ion-implantation machine at C.E.E.R.I., Pilani, on 0.2-0.6 ohm-cm, <111> oriented p-type substrate (V-1 to V-6). The implantation schedule was divided into two parts. In the first part, dose of the implanted boron ions was kept constant and energy was varied for each substrate where as in the second part energy was kept constant and dose was varied. The boron implantation Schedule is given in table 7 and 8.

After boron implantation in p-type silicon, oxide layer was grown on these samples by dry thermal oxidation method. Thermal oxidation was carried out at 950°C for two hrs in dry oxygen (1.0 lit/min). This low temperature oxidation was necessary to insure minimum effect on the implanted impurity profile distribution during oxidation process. Oxide layer thickness was measured by ellipsometer and was found to be 700Å. MOS capacitor were fabricated on these substrates and the high frequency C-V curves of each sample was plotted using C-V plotter model PAR 410. Fig 7 and Fig 8 show the experimental high frequency C-V plots for these samples. Threshold voltage is measured from the high frequency C-V curve, as shown in Fig 8 curve 1. Table 9 gives the value of threshold voltages calculated for various doses and energies from the experimental curves shown in Figs 7 and 8.

RESULTS AND DISCUSSIONS

Threshold voltage derived from equation 1 the numerical solution of Poisson's equation and from the method suggested by S.W. Tarasewicz et al are plotted in Figs.9 and 10 as a function of energy and dose Of implantation. Figs. 11 and 12 show the variation of average impurity concentration in maximum depletion layer width as a function of energy and dose of implanted ions. Figures 13 and 14 show the plots of maximum depletion layer width as a function of energy and dose. It is observed from Figures 10 and 11 that the results based on the numerical solution of Poisson's equations suggested by the authors and those based on the method suggested by S.W. Tarasewicz et. al. are reasonably close to each other. The experimental data, however, show some deviation from the theoretical curves. This could be because there may be some effect due to redistribution of impurities as the oxidation was done at 950 C° for two hours and oxide layer was grown on the implanted samples. Some implanted portion of the silicon

substrate was used up in the formation of silicon dioxide layer. Therefore, if we assume that the actual dopant profile in experimental sample may be approximately given by the L.S.S theory then the semiconductor surfaces of the MOS structure, fabricated in the manner described above, will correspond to a surface located at a depth of about 315Å of theoretical profile. Thus the values of surface concentration N_s and impurity concentration gradient M at the semiconductor surface of the experimental sample will actual be different from the model of MOS structure for which theoretical calculations for threshold voltage etc, have been made. There may be effect due to work function difference of metal and semiconductor and charge present in the oxide layer on the threshold voltage of MOS capacitor, the authors did not include while carrying out theoretical calculations. No attempts have been made by the authors, however, to carry out quantitative analysis of the deviation of experimental results from the theoretical ones in view of limitation of experimental facilities used.

The nature of variation in threshold voltage, obtained experimentally, with energy and dose of implantation is similar to those calculated theoretically. It is further observed that as the energy of the implanted boron ions is increased, keeping the dose fixed at 1×10^{14} ions/cm², the threshold voltage decreases as shown in Fig 9, where as when the dose of the boron implanted ions is increased, keeping the energy fixed at 50KeV, the threshold voltage increases, as shown in Fig.10. This variation of threshold voltage with energy and dose of implantation can be explained by studying the data shown in Figs 11 to 14. Figs.11 and 13 indicate that as the energy of the implanted ions increases, for a given dose, the maximum depletion width increases but the average impurity concentration within W_{max} decreases. The threshold voltage V_t of a MOS capacitor is dependent on the average impurity concentration N_{av} within the maximum depletion layer width, which decreases as the average impurity concentration decreases. From the above discussions, it is clear that as the energy of the implanted ions increases the threshold voltage decreases because of decrease in N_{av} . Increase of threshold voltage With increase of implanted ions dose, for a given energy, may be explained by studying the Figs. 13 and 14. These figures show that with increase in implantation dose the depletion width W_{max} decreases but the average impurity concentration within maximum depletion layer width increases. This means the threshold voltage will also increase with increase in dose, as seen in Fig.10

TABLE 1

Sr. No.	Energy(KeV)	Dose(atoms/cm ²)	R_p (micron)	ΔR_p (micron)
1	20	1×10^{14}	0.0662	0.0283
2	30	1×10^{14}	0.0987	0.0371
3	40	1×10^{14}	0.1302	0.0443
4	50	1×10^{14}	0.1608	0.0504
5	80	1×10^{14}	0.2465	0.0641
6	100	1×10^{14}	0.2994	0.0710
7	120	1×10^{14}	0.3496	0.0766

TABLE 2

Sr. No.	Energy(KeV)	Dose(atoms/cm ²)	R_p (micron)	ΔR_p (micron)
1	50	1×10^{12}	0.1608	0.0504
2	50	1×10^{13}	0.1608	0.0504
3	50	1×10^{14}	0.1608	0.0504
4	50	1×10^{15}	0.1608	0.0504

TABLE 3

Sr. No.	Energy (KeV)	Dose (ions/cm ²)	Threshold Voltage V_t (V)	W_{max} (cm)	N_{av} (atoms/cm ³)
1	20	1×10^{14}	26.12	2.287×10^{-6}	2.13×10^{18}
2	30	1×10^{14}	16.1	3.75×10^{-6}	1.23×10^{18}
3	40	1×10^{14}	11.39	4.381×10^{-6}	7.302×10^{17}
4	50	1×10^{14}	8.71	5.702×10^{-6}	3.73×10^{17}
5	80	1×10^{14}	4.55	9.809×10^{-6}	1.32×10^{17}
6	100	1×10^{14}	3.6	1.101×10^{-5}	9.04×10^{16}
7	120	1×10^{14}	2.89	1.449×10^{-5}	5.64×10^{16}

TABLE 4

Sr. No.	Energy (KeV)	Dose (ions/cm ²)	Threshold Voltage V _T (V)	W _{max} (cm)	N _{av} (atoms/cm ³)
1	50	110 ¹²	2.96	1.59x10 ⁻⁵	3.18x10 ¹⁶
2	50	110 ¹³	4.86	1.06 x10 ⁻⁵	1.615 x10 ¹⁷
3	50	110 ¹⁴	8.71	5.702 x10 ⁻⁶	3.73 x10 ¹⁷
4	50	110 ¹⁵	18.44	3.00 x10 ⁻⁶	1.59 x10 ¹⁸

TABLE 5

Sr. No.	Energy (KeV)	Dose (ions/cm ²)	M (atom/Cm ⁴)	N _s (atoms/cm ³)	W _{max} (cm)	N _{av} (atoms/cm ³)	V _T (volts)
1	20	110 ¹⁴	2.078x10 ²⁴	2.38x10 ¹⁷	2.078x10 ⁻⁶	2.86x10 ¹⁸	23.8
2	30	110 ¹⁴	6.83 x10 ²³	4.659 x10 ¹⁷	2.966 x10 ⁻⁶	1.059 x10 ¹⁸	15.79
3	40	110 ¹⁴	4.02 x10 ²³	-1.52 x10 ¹⁷	3.743 x10 ⁻⁶	6.017 x10 ¹⁷	11.58
4	50	110 ¹⁴	1.61 x10 ²³	-8.76 x10 ¹⁶	5.035 x10 ⁻⁶	3.192 x10 ¹⁷	8.47
5	80	110 ¹⁴	4.17 x10 ²²	-7.257 x10 ¹⁶	8.26 x10 ⁻⁶	1.061 x10 ¹⁷	4.74
6	100	110 ¹⁴	2.89 x10 ²²	-6.92 x10 ¹⁶	9.57 x10 ⁻⁶	6.96 x10 ¹⁶	3.95
7	120	110 ¹⁴	1.30 x10 ²²	-3.80 x10 ¹⁶	1.225 x10 ⁻⁵	4.187 x10 ¹⁶	3.19

TABLE 6

Sr. No.	Energy (KeV)	Dose (ions/cm ²)	M (atom/Cm ⁴)	N _s (atoms/cm ³)	W _{max} (cm)	N _{av} (atoms/cm ³)	V _T (volts)
1	50	110 ¹²	5.29x10 ²¹	-1.033x10 ¹⁶	1.51x10 ⁻⁵	2.98x10 ¹⁶	2.87
2	50	110 ¹³	4.64 x10 ²²	-8.617x10 ¹⁶	8.11 x10 ⁻⁶	1.02 x10 ¹⁷	4.74
3	50	110 ¹⁴	1.61 x10 ²³	-8.76x10 ¹⁶	5.035 x10 ⁻⁶	3.19 x10 ¹⁷	8.47
4	50	110 ¹⁵	1.27 x10 ²⁴	-3.21 x10 ¹⁷	2.58 x10 ⁻⁶	1.32 x10 ¹⁸	17.19

TABLE 7

Sr. No.	Sample No.	Energy (KeV)	Dose (ions/cm ²)
1	V-1	50	1X10 ¹⁴
2	V-2	80	1X10 ¹⁴
3	V-3	100	1X10 ¹⁴
4	V-4	120	1X10 ¹⁴

TABLE 8

Sr. No.	Sample No.	Energy (KeV)	Dose (ions/cm ²)
1	V-5	50	1X10 ¹²
2	V-6	50	1X10 ¹³
3	V-1	50	1X10 ¹⁴

TABLE 9

Sr. No.	Sample No.	Energy (KeV)	Dose (ions/cm ²)	Threshold Voltage V _T (V)
1	V-5	50	1X10 ¹²	2.1
2	V-6	50	1X10 ¹³	3.1
3	V-1	50	1X10 ¹⁴	8.0
4	V-2	80	1X10 ¹⁴	7.5
5	V-3	100	1X10 ¹⁴	6.2
6	V-4	120	1X10 ¹⁴	5.7

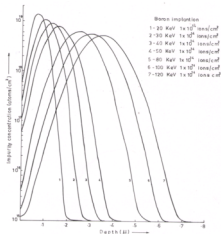


FIG. 1 IMPURITY CONCENTRATION PROFILES FOR VARIOUS ENERGIES AND FIXED DOSE.

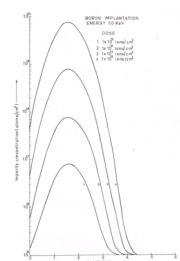


FIG. 2 IMPURITY CONCENTRATION PROFILES FOR VARIOUS DOSES AND FIXED ENERGY.

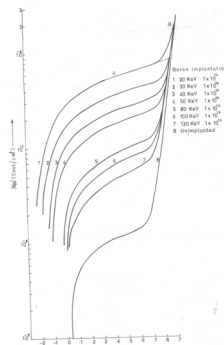


FIG. 3 VARIATION OF SPACE CHARGE DENSITY AS A FUNCTION OF SURFACE POTENTIAL.

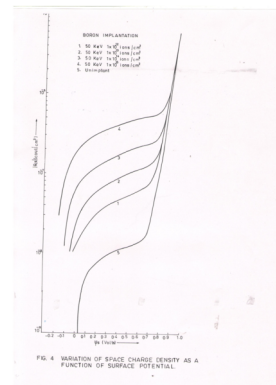


FIG. 4 VARIATION OF SPACE CHARGE DENSITY AS A FUNCTION OF SURFACE POTENTIAL.

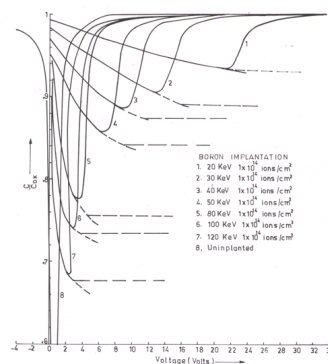


FIG. 5(a) C-V CURVES CALCULATED FOR THE PROFILES OF FIG. 1. DETAILS OF CURVE 8 SHOWN IN FIG. 5(b)

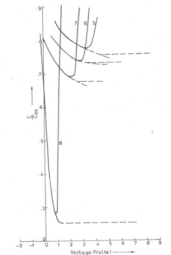


FIG. 9 (b) DETAILS OF CURVE 8 SHOWN IN FIG. 9(a)

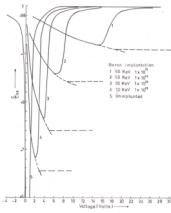


FIG. 9 (c) C-V CURVES CALCULATED FOR THE PROFILES OF FIG. 7. DETAILS OF CURVE 5 SHOWN IN FIG. 6(a)

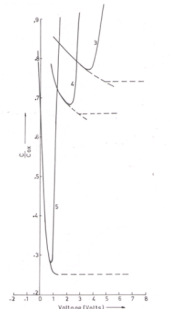


FIG. 9 (d) DETAILS OF CURVE 5 SHOWN IN FIG. 6(b)

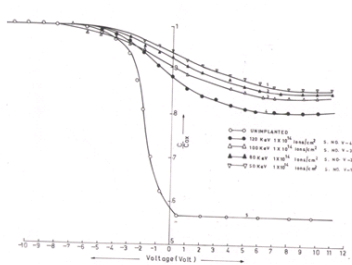


FIG. 7 EXPERIMENTAL C-V CURVES FOR VARIOUS ENERGIES AND FIXED DOSE.

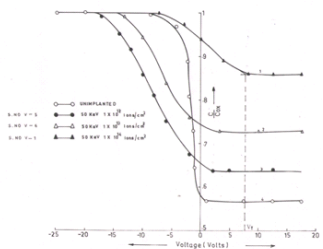


FIG. 8 EXPERIMENTAL C-V CURVES FOR VARIOUS DOSES AND FIXED ENERGY.

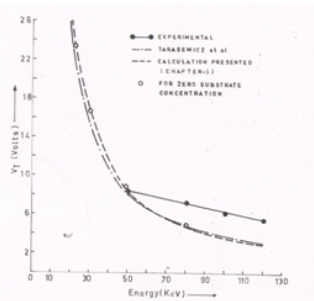


FIG. 9 THRESHOLD VOLTAGE AS A FUNCTION OF ENERGY.

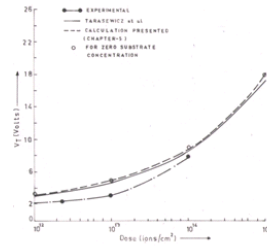


FIG. 10 THRESHOLD VOLTAGE AS A FUNCTION OF DOSE.

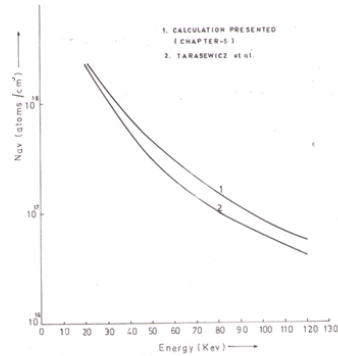


FIG. 11 AVERAGE IMPURITY CONCENTRATION AS A FUNCTION OF ENERGY, FIXED DOSE - 1×10^{17} ions/cm²

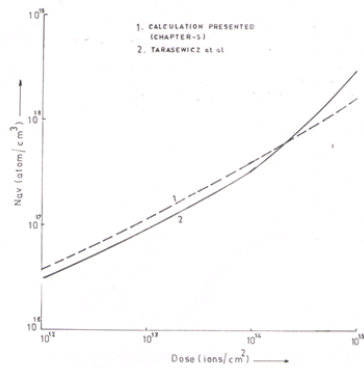


FIG. 12 AVERAGE IMPURITY CONCENTRATION AS A FUNCTION OF DOSE, FIXED ENERGY 50 KeV.

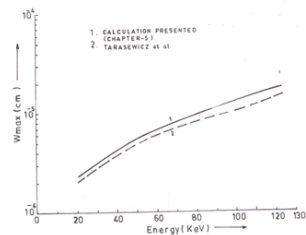


FIG. 13 MAXIMUM DEPLETION LAYER WIDTH AS A FUNCTION OF ENERGY, FIXED DOSE 1×10^{17} ions/cm².

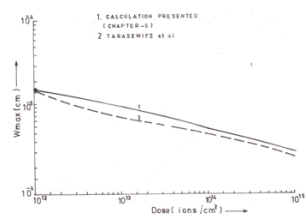


FIG. 14 MAXIMUM DEPLETION LAYER WIDTH AS A FUNCTION OF DOSE, FIXED ENERGY 50 KeV.

REFERENCES

- 1) K.H. Nicholas, Radiation effects, 28,(1976)177.
- 2) Anil Kumar, G.S. Virdi, P.J. George, S.K. Chattopadhyaya and N.Nath, 8th Conf. Applic. Res. and Industry, Denton, USA, Poster Paper (Nov. 1984), p.256.
- 3) Anil Kumar, G.S. Virdi, P.J. George, S.K. Chattopadhyaya and N.Nath, Microelectronics Journal, 29(1998) 299-305.
- 4) S.D. Brotherton and P. Burton, Solid state electron, 133,(1970)1591.
- 5) M.R. Macpherson, solid state electron, 15, (1972)1319.
- 6) M.R. Macpherson, Appl. Phys. Lett., 18,(1971)502.
- 7) G. Doucet and F. Van De Wiele, Solid State Electron, 16, (1973)417.
- 8) E.C. Douglas and A.G.F. Dingwall, IEEE Trans. Electron Device, ED-21,(1974)324.
- 9) R.R. Troutman, IEEE Trans. Electron Devices, ED-24,(1977)182.
- 10) J.R. Brew, IEEE Trans. Electron Devices, ED-26,(1979)1696.
- 11) S.W. Tarasewicz and C.A.T. Salama, Solid State Electron, 27, (1984)33.
- 12) M.L. James, G.M. Smith and J.C. Walford, 'Applied Numerical Methods for Digital Computation', Third Edition, Harper and Row Publisher, New York.
- 13) P. Richwan, 'MOS Field-effect Transistors and Integrated Circuits', A Wiley-Interscience Publication Co., New York.
- 14) W.E. Beadle, J.C.C. Tsai and R.D. Plummer, 'Quick References Manual for Silicon Integrated Circuit technology', pp.7-6, A Wiley-Interscience Publication, John Wiley and Sons., New York.
- 15) J. Lindhard, M. Scharff and H.E. Schioff, Kgl. Danske Videnskab Selskab, Mat-Medd., 33, 14(1963).